

## RED WATER AND DISCOLORATION IN A WDS: A NUMERICAL SIMULATION

Naser G.<sup>1</sup>, Karney B. W.<sup>2</sup>, and Boxall J. B.<sup>3</sup>

<sup>1</sup> Ph.D. Candidate, Civil Eng. Dept., Univ. of Toronto, Canada, [gnaser@ecf.utoronto.ca](mailto:gnaser@ecf.utoronto.ca)

<sup>2</sup> Professor, Civil Eng. Dept., Univ. of Toronto, Canada, [karney@ecf.utoronto.ca](mailto:karney@ecf.utoronto.ca)

<sup>3</sup> Associate Professor, Civil Eng. Dept., Univ. of Sheffield, UK, [j.b.boxall@sheffield.ac.uk](mailto:j.b.boxall@sheffield.ac.uk)

### Abstract

*Discoloration is a major source of consumer complaints associated with a water distribution system (WDS). Depending on the pipe material, different colors can be attributed to varying concentrations and chemical oxidation states of iron or other metals. Overall, the discoloration materials are apparently entrained from particles at the pipe wall during the passage of water. The major material sources for discoloration materials are organic and inorganic materials entering a WDS at the source, materials from treatment processes, processes within a WDS such as corrosion and erosion, biological growth and chemical reactions, external contamination occurring during operations and repairs, intrusion and back flow. Traditionally, two mechanisms – hydraulic entrainment and iron uptake – have been used to describe discoloration events. The hydraulic-entrainment mechanism is the physical motion of loose deposits of particles at the pipe wall into the bulk flow due to abrupt changes in the flow condition. In iron-uptake mechanism, some particles of ferrous hydroxide (produced by corrosion reactions) are oxidized to ferric hydroxide, which then can cause red bulk events in the bulk flow.*

*Considering the hydraulic-entrainment a key main mechanism initiating discoloration event, this paper seeks in at least a preliminary way to simulate and approximate red water events in a water a WDS. Abrupt changes in flows can create aggressive shear forces, sometimes causing the accumulated particles at the pipe wall to be resuspended and be carried with the bulk flow. In this study, one- and two-dimensional (1-D and 2-D) transient simulation models are proposed, by which the turbidity of water is modeled with a transport equation. The transport equation, which is then coupled with the appropriate continuity and momentum equations for flow, considers advection and diffusion as the main mass transport mechanisms. Defining a self-cleaning threshold limit for wall shear stress, Boxall's approach is used here to model the release of the discoloration material from the pipe wall into the bulk flow.*

*To overcome the complexity in the determination of the turbulent shear stresses and to reduce the computational burden, a five-region model is used to model the turbulence. In this model, molecular viscosity is responsible for damping turbulence in the region near the pipe wall (viscous sublayer) while eddy viscosity is the main damping-mechanism in the core region (nearer the centerline of the pipe). The turbulent diffusivity coefficient is accurately approximated from the eddy-diffusivity concept and the dimensionless turbulent Schmidt number; whereas the 1-D counterparts are determined using steady state Darcy-Weisbach formula (for wall shear stress) and Taylor's formula (for diffusion coefficient). An implicit/explicit finite difference method; namely an Alternating Direction Implicit (ADI) approach, is superposed with a fixed grid method of characteristic (MOC) to numerically integrate the governing equations for unknown flow parameters including velocity, pressure head, and water turbidity. Finally, the results of both 1-D and 2-D models for a straightforward reservoir-pipe-valve case study are compared with available field data reported in the literature by other researchers. The overall agreement of the two sets of results supports the basic validity of the proposed 1-D and 2-D models.*

**Keywords:** Red Water, Discoloration, Wall Shear Stress, Transient Flow.

## 1. INTRODUCTION

Discoloration, occasionally observed and caused by rust, is one of the major sources of consumer complaints associated with a WDS. Different colors can be attributed to varying concentrations and chemical oxidation states of iron or other metals (depending upon the pipe material). In areas of little flow where aging pipes contribute rust and sediment, discoloration of the water can occur. If an unusually large flow of water is experienced in the main (due to a broken pipe, repairing or replacing a water main, operating a fire hydrant, or system flushing), sediments can become dislodged and temporarily suspended in the water imbuing with a certain hue. In fact, significant flow changes produce aggressive shear forces at the pipe wall that can cause the accumulated material to be mobilized and possibly delivered to the consumer's tap. Thus, the determination of the aggressive shear-force and the resistance of accumulated layer against this force is the key step in investigating the discoloration event. This simply means that the discoloration materials are originally stable in their positions at the pipe wall and become mobilized only if the driving force exceeds the resistance of the stable material. However, due to improvements in water treatment technology, treatment has less influence on discoloration events (Boxall et al., 2001).

Overall, the discoloration materials are apparently entrained during the passage of water in a WDS, and find their origin in corrosion products at the pipe wall. The major material sources for discoloration events (WRc, 1989) are usually considered as organic and inorganic materials entering a WDS at the source, materials from treatment processes, processes within a WDS such as corrosion and erosion, biological growth and chemical reactions, external contamination occurring during operations and repairs, intrusion and back flow. Predictive modeling of discoloration events is significant since it could be used to optimize the operation and maintenance of a WDS and also to minimize the water turbidity, the discolored-water-event return frequency, and therefore customer complaints. In other words, there could be a cost savings and reduced customer complaints if the location, severity, timing, and risk of discoloration events within a WDS are better managed.

## 2. BACKGROUND

As Boxall et al. (2001) argued, discoloration events are rarely due to color inducing compounds in solution, but rather suspended materials within the flow. There are a variety of sources that may cause discoloration events with the antecedent responsible mechanisms being relatively complex and dependent on system and material characteristics, which are typically unknown, uncertain, or hard to measure. Nonetheless, two mechanisms have been traditionally considered for describing the discoloration events: hydraulic-entrainment and iron-uptake mechanisms.

### *2.1 Hydraulic Entrainment Mechanism*

As Hoven et al. (1994) suggested, hydraulic entrainment involves the movement of loose deposits of particles at the pipe wall into the bulk flow due to abrupt changes in the flow condition. The abrupt change creates an aggressive shear force causing the particles to be resuspended and carried with the bulk flow. Through field investigation, Hoven et al. (1994) observed irregular day-time peaks for water turbidity. Considering the fact that the peak water demands are in day-time, the irregular peaks are associated with the resuspension of loose

particles. Such a sequence of irregular peaks was not observed during the night-time turbidity pattern.

## ***2.2 Iron-Uptake Mechanisms***

Some other studies suggest that red water materials do not include crystalline particles of corrosion products, but rather flocs of ferric hydroxide (AWWARF, 1996). Diffusing into the bulk flow, some particles of ferrous hydroxide, produced by corrosion reactions, are oxidized to ferric hydroxide, which occur as red water materials (Wagner and Kuch, 1984). According to Kuch and Sontheimer (1986), regular changes from stagnation to flow are the key factor in the iron-uptake mechanism as it diffuses more oxygen and therefore increases the oxidation rate of ferrous iron. According to Kuch (1984), the corrosion continues even when the oxygen is completely depleted during a stagnation period. In this case, ferric oxides assume the role of the depleted oxidant in the water (AWWARF, 1996).

## ***2.3 Numerical Models***

The occurrence of red (or ochre) water has been under investigation since the beginning the 19<sup>th</sup> century when Baylis (1926) studied corrosion and red water events by determining of the role of bacteria in iron corrosion and tubercle formation. Recent works by Hoven and Vreeburg (1992), Woodward et al. (1995), Smith et al. (1996, 1997, and 1999) clarified the physical descriptions of discoloration events. However, until Boxall et al. (2001), there was almost no attempt to hydraulically understand study discoloration events.

Boxall et al. (2001) developed a three-step novel approach to modeling sediment movement in distribution mains based on particle characteristics. They considered the size and the relative density of the particles and hypothesized that the discoloration materials are produced due to erosion of the corrosion layers (the erosion step), which are then transported by the bulk flow (the suspension step), although some parts of the suspended loads may resettle on the pipe wall (the regeneration step). In essence, their model was based on a change in the layer strength with the degree of erosion.

More recently, through an incorporation of this understanding into a water quality model for a case study in the UK, Boxall et al. (2003) demonstrated the potential of the approach to predict the occurrence of discoloration events in a real WDS. The predicted results illustrated the same pattern as the measured field-data for turbidity. An increase in turbidity due to flushing followed by an exponential decay in water turbidity was well recognized both in the field data and in the model predictions, which at least partially confirms the applicability of the approach for management and operational purposes. The study concluded with the following findings:

- Exponential decay generally supports the cohesive-like nature of the discoloration materials, which exist in variable strength layers on the pipe walls within the WDS,
- The progressive accumulation of water turbidity along the pipe length evinces a uniform distribution for cohesive layers in the pipe,
- There is no apparent relation between the pipe material, age, flushing hydraulics and the characteristics of the mobilized material.

One challenge is that Boxall's model involves a set of empirical and highly problem-dependent parameters, which are largely unknown for a WDS. These parameters must be determined through careful calibration.

In the current study, a 2-D numerical model is used to couple a mass transport equation (including advection and diffusion) for the water turbidity (resulting from the particles resuspension at the pipe wall) with a comprehensive model for flow. In this way, using the modified Vardy-Hwang model, a 2-D hydraulic model for transient flow is further coupled with a 2-D mass transport equation.

This numerical coupling of the flow equations is accomplished by introducing two different approximation schemes; one for the mass transport and the other for the system hydraulics. Therefore, in this study, a finite difference method (FDM) is used to numerically integrate the mass transport equation and MOC to integrate the continuity and momentum equations. Considering different mechanisms responsible for damping the turbulence along the pipe section, and to overcome the complexity in the determination of the turbulent shear stresses and to reduce computational burden, the standard five-region turbulence model is used to model velocity fluctuations. Finally, the numerical results of the proposed 2-D model for a reservoir-pipe-valve case study of a WDS in the UK are compared with the corresponding available field data in the literature.

### 3. MATHEMATICAL MODEL

#### 3.1 Flow Equations

Considering the fact that resuspension of loose deposits of solid particles from the pipe wall into the bulk flow is the primary mechanism of the red water occurrence and the significant role of abrupt changes in flow conditions, a more precise modeling of system hydraulics is crucial. This is mathematically modeled using the modified Vardy & Hwang (1991) described by:

$$\frac{g}{a^2} \frac{\partial H}{\partial t} + \frac{\partial U}{\partial x} + \frac{1}{r} \frac{\partial}{\partial r} (rV) = 0 \quad (1)$$

$$\frac{\partial U}{\partial t} + g \frac{\partial H}{\partial x} = \frac{1}{r\rho} \frac{\partial}{\partial r} (r\tau) \quad (2)$$

in which  $x$ ,  $r$  are the distances in longitudinal and radial directions,  $t$  is the time,  $U$  and  $V$  are the components of the time-averaged local velocity in longitudinal and radial directions,  $H$  is the piezometric head,  $\rho$  is the fluid density,  $\tau$  is the shear stress,  $g$  is the gravitational acceleration, and  $a$  is the wave speed.

Using time averaging, the turbulent shear stress can be expressed as:

$$\tau = \rho \nu_m \frac{\partial U}{\partial r} - \overline{\rho uv} = \rho (\nu_m + \nu_t) \frac{\partial U}{\partial r} \quad (3)$$

where  $u$  and  $v$  are the turbulence fluctuations of velocity in the longitudinal and radial directions, and  $\nu_t$  and  $\nu_m$  are kinematic turbulent and molecular viscosity coefficients. More details on the hydraulic model and its numerical solution are given in Zhao and Ghidaoui (2003).

### 3.2 Turbulence Modeling

The Reynolds shear stress term,  $-\overline{\rho uv}$ , in (2) and (3) can readily be calculated using the eddy viscosity concept. In principle, the model can be used with any prescribed turbulence model for the eddy viscosity concept. However, to overcome the complexity in the determination of the turbulent shear stresses and to reduce the computational burden, the standard five-region turbulence model, initially proposed by Kita et al (1980), is used in this study to model velocity fluctuations. This approach is justified by the fact that different mechanisms are responsible for damping the turbulence along the pipe section. In fact, molecular viscosity is dominant in the region near to the pipe wall (viscous sublayer) while eddy viscosity is the main damping-mechanism in the core region (close to the centerline of the pipe).

More clearly, the cross section of the pipe is divided into five flow-regions, namely viscous layer (next to the pipe wall), buffer layer I, buffer layer II, logarithmic region, and the core region (at the pipe centerline). An algebraic model for turbulent viscosity corresponding to each layer is thus expressed as follows:

$$\text{Region 1 (Wall Region): } 0 < y^* < \frac{1}{\beta} \quad \frac{v_T}{v_m} = 1.0 \quad (4)$$

$$\text{Region 2: } \quad \frac{1}{\beta} < y^* < \frac{\beta}{C_b} \quad \frac{v_T}{v} = \beta y^* \quad (5)$$

$$\text{Region 3: } \quad \frac{\beta}{C_b} < y^* < C_{c_2} \quad \frac{v_T}{v} = C_b y^{*2} \quad (6)$$

$$\text{Region 4: } \quad C_{c_2} < y^* < C_{c_3} \quad \frac{v_T}{v} = \kappa y^* \left( 1 - \frac{\kappa y^*}{4C_m R_e^*} \right) \quad (7)$$

$$\text{Region 5 (Core Region): } C_{c_3} < y^* < R_e^* \quad \frac{v_T}{v} = C_c R_e^* \quad (8)$$

in which  $v_T$  is the total viscosity;  $R_e^* = UR/v_m$ ;  $U^* = \sqrt{\tau_w/\rho}$ ;  $y^* = U^* y/v_m$ ; and  $y$  is the distance from the pipe wall. The values for the numerical coefficients, proposed by Kita et al (1980), are:  $\beta = 0.19$ ,  $C_b = 0.011$ ,  $C_m = 0.077$ , and  $\kappa = 0.41$ . The parameter  $C_c$  is in general a function of Reynolds number and typically lies in the range 0.05-0.07. The coefficients  $C_{c_2}$  and  $C_{c_3}$  in (3-24) and (3-25) are expressed as:

$$C_{c_2} = \frac{\kappa}{C_b + \left( \frac{\kappa^2}{4C_m R_e^*} \right)} \quad (9)$$

$$C_{c_3} = \frac{2C_m R_e^*}{\kappa} \left( 1 + \sqrt{1 - \frac{C_c}{C_m}} \right) \quad (10)$$

Since the most rapid changes in the velocity profile occur in the regions adjacent to the pipe wall, these regions are much more important than the others.

### 3.3 Mass Transport Model

A clear understanding of the transport of particles in the radial direction is an important prerequisite to the modeling of discoloration events in a WDS. Clearly, the dominant mechanism responsible for this distribution is advection in the flowing water and consequently the aggressive shear force that it exerts at the pipe wall. In general, the extent of this mechanism depends upon many factors including flow conditions, the resistance of accumulated materials at the pipe wall, the material and age of the pipe. Therefore, applying the mass conservation law, the unsteady transport PDE governing the turbidity of water in the system is obtained as:

$$\frac{\partial C}{\partial t} + U \frac{\partial C}{\partial x} + V \frac{\partial C}{\partial r} = \frac{\partial}{\partial r} \left( \Gamma \frac{\partial C}{\partial r} \right) + \frac{\partial}{\partial r} \left( r \Gamma \frac{\partial C}{\partial r} \right) \quad (11)$$

in which  $C$  is water turbidity (NTU) at point  $(x, r)$  and time  $t$  and  $\Gamma$  is total diffusion coefficient defined by turbulent ( $\Gamma_t$ ) diffusion and its molecular ( $\Gamma_m$ ) counterpart. According to Rodi (1993), using the Reynolds analogy between mass and momentum transport, the turbulent diffusivity coefficient is accurately approximated from the eddy-diffusivity concept and the dimensionless turbulent Schmidt number.

Neglecting the effects of molecular transport, the turbulent Schmidt number expresses the quantitative difference between the turbulent material (or heat) transport rate and momentum in turbulent flows. The turbulent Schmidt number, comparing the eddy viscosity of the turbulent flow with the eddy material diffusivity, is thus supposed to be around unity. Despite this, it has been argued that the turbulent Schmidt number manifests only small variations across any flow, and also from flow to flow (Rodi, 1993). Consequently, as is done in many other mathematical models, the turbulent Schmidt number was considered invariable throughout this study. In fact, the assumption of using a constant turbulent Schmidt number across the whole flow field implies a similar relationship between the momentum and material transport processes irrespective of the turbulence structure. This has been questioned recently for various flow scenarios.

## 4. NUMERICAL SOLUTION

A numerical model should not only be consistent, stable, and convergent to an accurate solution, but it should also be easy to use, modify, implement, and efficient in terms of computational time and computer memory requirements (Abbott and Minns 1998). Efficient schemes minimize the computer processing time and memory requirements; although recent advances in computer technology render the memory requirement less stringent, a technique that is more memory efficient can still be used to solve larger problems. One of the mathematically interesting parts of water quality simulation arises from the hyperbolic and parabolic nature of the PDEs describing flow hydraulics and mass transport mechanisms, respectively. The numerical challenge, in this study, is to integrate the transport equation of (11) with a finite difference-based scheme (e.g., Alternating Direction Implicit approach, ADI) and the flow equations of (1) and (2) using the Method of Characteristics (MOC).

## 5. BOUNDARY AND INITIAL CONDITIONS

As is the case for any set of differential equations, boundary conditions are necessary to solve the system of equations given by (1), (2), and (11). On the other hand, the exact values of input parameters and boundary conditions for most engineering problems are seldom known exactly. Thus, the effects of these variations should be considered thoroughly. To study the water quality model, the turbidity concentration must be specified at the boundaries (boundary conditions) and at the beginning of the simulation (initial conditions) as follows:

### 5.1 Boundary Conditions

These include water turbidity at the inlet and outlet sections together with that at the pipe centerline and wall.

- Upstream (inlet) section: This was considered as the boundary with turbidity:

$$C(x = 0, r, t) = C_{in} \quad (12)$$

- Downstream (outlet) section: It is modeled as a no-flux boundary. Hence:

$$\left. \frac{\partial C}{\partial x} \right|_{x=L,r} = 0 \quad (13)$$

- Pipe-Wall Boundary: This is simply studied through the discoloration model described by Boxall et al. (2001). The model is based on a cohesive transport theory. Defining a self-cleaning threshold limit for wall shear stress, the discoloration model used in this study is entirely based on Boxall's three-step approach. Considering erosion, suspension, and regeneration as the main causes for the release of materials from the pipe wall, they showed that even the most quiescent conditions in a WDS are sufficient to carry all the materials as a persistent suspension wash load. Hence, ignoring the regeneration of the materials (due to accumulation), the discoloration model can be described as:

$$\tau_s = \frac{C^b - C_{max}}{k} \quad (14)$$

in which  $\tau_s$  is the corrosion layer yield strength;  $C$  is a measure of the turbidity potential of the layer;  $C_{max}$  represents an upper limit for the stored turbidity of the layer;  $k$  is the gradient describing the relationship between the yield strength and the ability of the corrosion layer to increase turbidity; and  $b$  is a dimensionless power term.

Defining  $R_s$  as the rate of supply from the corrosion layer, the mobilization of the cohesive layers is described as:

$$R_s = \frac{P(\tau_a - \tau_s)^n}{Q} \quad (15)$$

in which  $\tau_a$  is the available shear stress at the pipe wall;  $Q$  is the flow discharge; the coefficient  $P$  and the dimensionless exponent  $n$  are used to describe the eroding forces at the pipe wall.

The removed materials by excess shear force at the pipe wall are then washed away with the bulk flow and carried along the pipeline. Thus, the change in water turbidity ( $\Delta C$ ) due to the passage of flow can be obtained by multiplying the supply rate by the internal surface area of the pipe length swept as:

$$\Delta C = R_s \times A_s \quad (16)$$

in which  $A_s$  is the pipe surface-area swept in the time step under consideration.

The parameter  $R_s$  is used to calculate the change in the stored turbidity and also to update the strength of the layer for the next time-step. Considering the fact that flow discharge through the pipe is known over a discrete water quality time-step ( $\Delta t_{wq}$ ), the change in the stored turbidity ( $\Delta C$ ) of the layer is determined as:

$$\Delta C = R_s \times Q \times \Delta t_{wq} \quad (17)$$

Unfortunately, the parameters  $P$ ,  $n$ ,  $b$ ,  $k$ , and  $\tau_s$  are truly problem dependent and they must be determined through a careful calibration procedure.

- Pipe-Centerline Boundary: This is simply considered as a no-flux boundary for water turbidity. Hence:

$$\left. \frac{\partial C}{\partial r} \right|_{x, r=0} = 0 \quad (18)$$

### 5.2 Initial Conditions

This includes the turbidity at the time before flushing starts, which is set as constant turbidity in this study:

$$C(x, r, t = 0) = C_o \quad (19)$$

## 6. SYSTEM CHARACTERISTICS AND CASE STUDY

In order to assess the validity of the proposed model, a reservoir-pipe-valve case drawn from Boxall et al. (2001), is studied here. As it is given in Fig. 1, the system includes a pipeline with 1600 m length, 65 mm diameter, and an estimated 5.5 mm internal roughness connected to a constant-head reservoir with a water surface elevation of 64 m (above the pipe's centerline) at the upstream end and to a valve (with a known loss coefficient) at the downstream end and with a valve-coefficient of  $0.00152 \text{ m}^{2.5}/\text{s}$ . The normal daily flow rate is in the range of 0.04-0.22 liter/s (considered as 0.2 liter/s in this study). The valve is completely opened in an instant to

produce a final flushing discharge of 2.4 liter/s during which clean water with no turbidity is continuously supplied at the upstream end. The initial water turbidity is also assumed as zero. The turbidity was calculated at the valve-position.

Although considerable details of the case study are given in Boxall et al. (2001), not all of the system's data are mentioned in the original article. Thus, Dr. Joby B. Boxall was consulted directly (November 2004).

For the purpose of stability and accuracy of the numerical simulation, the pipe was divided into 400 reaches ( $N_x=400$ ) in the longitudinal direction (for both 1-D and 2-D models) and 300 cylinders ( $N_r=300$ ) in the radial direction (for the 2-D model only). Considering the Courant condition for stability ( $C_r=1.0$ ), the time-step for the transient flow simulation ( $\Delta t_{tf}$ ) was 0.007s for both the 1-D and 2-D models. Regarding the accumulation term, the ratio of the time-steps for hydraulic and discoloration analysis ( $\Delta t_{wq}/\Delta t_{tf}$ ) were set as 50 and 2 for the 1-D and 2-D models, respectively. To facilitate the comparison between the numerical results and field data, all the local flow parameters of the 2-D simulation are again averaged over the cross-sectional area of the pipe.

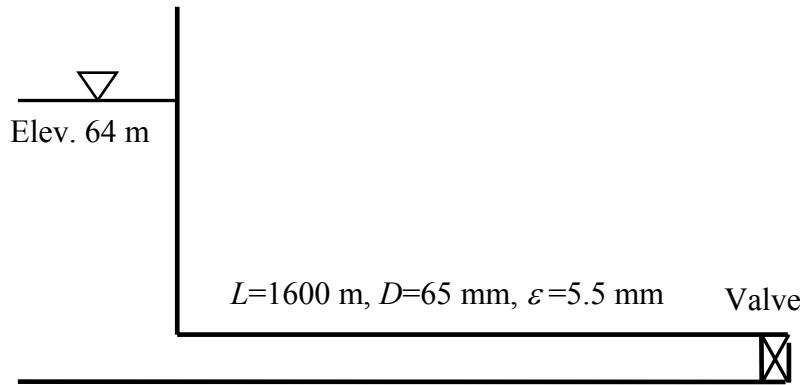


Fig. 1 – Schematic of the pipe system for the case study

## 7. MODEL APPLICATION AND RESULTS

The results of the 1-D and 2-D simulations for system hydraulics and water turbidity are compared with the available field data in Fig. 2 through Fig. 7. These are discussed in more detail in the following sections.

Fig. 2 demonstrates the system response (from both the 1-D and 2-D models) for the pressure head at a typical section at the middle of the pipe ( $x=800$  m). Overall, following the valve opening, the flow accelerates and simultaneously causes a decrease in pressure. The pressure wave then travels up and down through the system until it decays under the effects of friction and shear stress, gradually approaching a new steady-state condition. Surprisingly, however, the Figure indicates a higher pressure-head variation for the 2-D analysis than that of the 1-D model. The significant difference in pressure head predictions is in fact due to a higher production of energy dissipation by the steady state formula (Darcy-Weisbach equation in this study) in 1-D analysis than that of the five-region model in the 2-D approach, which is well represented in Fig. 3. The Figure displays the variation of the wall shear stresses at a section at the middle of the pipe. Moreover, the absolute pipe-wall roughness of 5.5 mm for the current

pipeline system and the corresponding friction factor of 0.1, produce relatively high shear stresses at the pipe wall, which are much larger than those obtained by the standard five-region turbulence model. Considering the fact that the aggressive shear forces have critical role in resuspending the particles from pipe wall into the bulk flow via (15), this highlights the need for a better turbulence model that more directly considers the internal wall-roughness of the pipe.

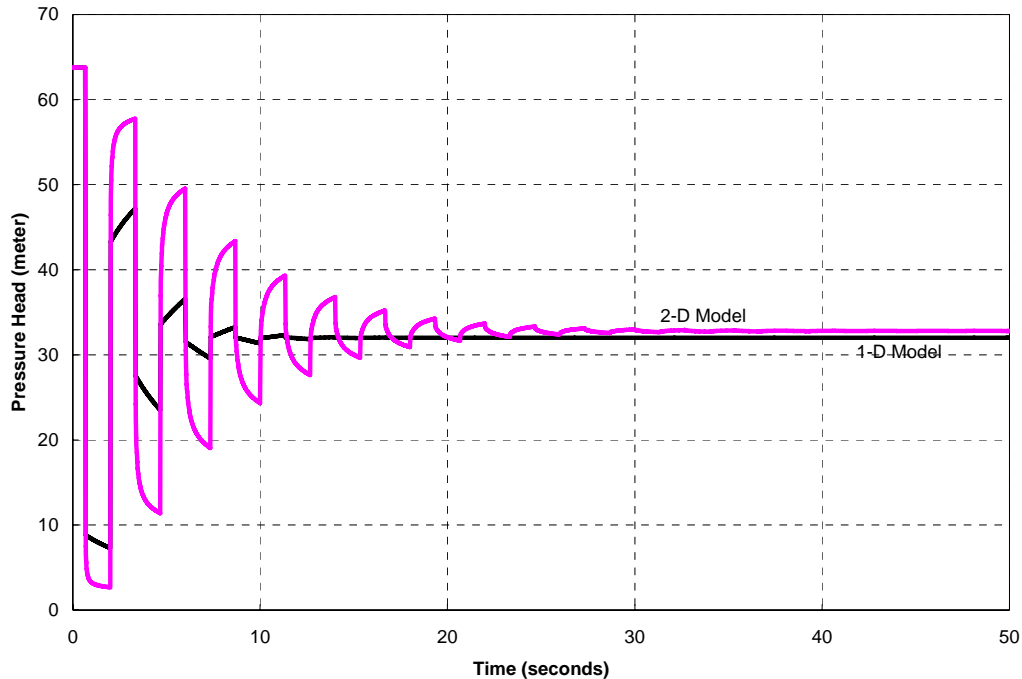


Fig. 2 – Pressure variation at the middle of the pipe calculated by the standard five-region turbulence model for the 2-D approach

One way is to adjust the standard values of the parameters in the five-region model in a way that produces significantly higher energy dissipation. Such an adjustment was conducted on the standard five-region turbulence model by increasing the coefficient  $\beta$  of the five-region turbulence model from a standard value of 0.19 to an adjusted one of 1.5. The results of the adjusted 2-D model compared with those of the 1-D are given in Figs. 4 and 5 for the pressure head and wall shear stresses at the middle of the pipe. The Figures clearly reveal excellent agreement between the adjusted results. Unfortunately, however, the difficulty with this correction is that the effective values of the turbulence-model's parameters cannot easily be estimated in advance for a real problem. Moreover, this kind of adjustment may cause discontinuity in the radial distribution of the eddy viscosity at the regions' interfaces, which consequently produces more error. As a result, considering the effect of wall roughness, a more realistic turbulence model (perhaps a  $k-\varepsilon$  model) could predict more accurately the energy dissipation and therefore shear stresses.

Fig. 6 depicts flow discharge variation at the section at the middle of the pipe with time. Interestingly, as the Figure shows, the results of the 1-D analysis exhibit a temporary increase in flow discharge (a bit more than the 2.4 liter/s) around 4 s after valve opening as a result of compressibility and inertia. Generally, as is clear from Figs. 2 to 6, it takes approximately 15 s (based on the 1-D and adjusted 2-D simulations) for the system to reach the new steady state

flow discharge of 2.4 liter/s. In contrast, the time corresponding to the standard 2-D analysis is almost 30 s when the system approaches relatively a final steady state condition.

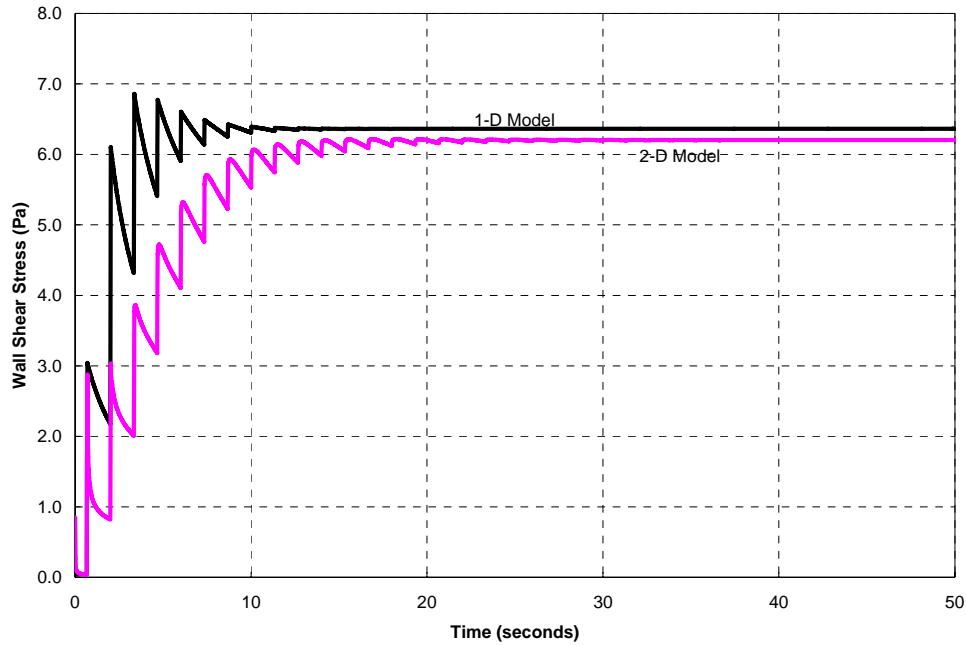


Fig. 3 – Wall shear stress at the middle of the pipe calculated by the standard five-region turbulence model for the 2-D approach

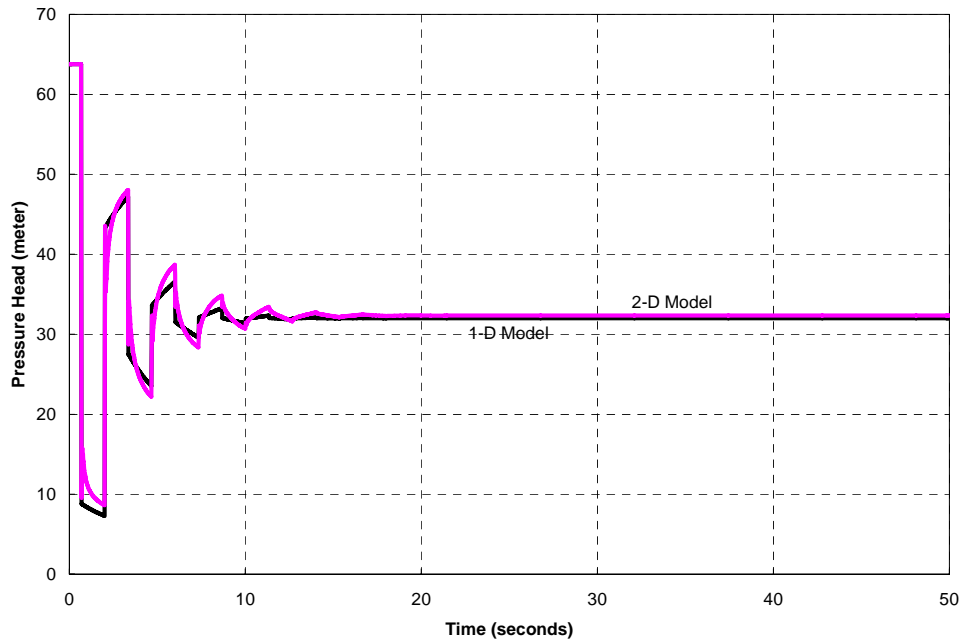


Fig. 4 – Pressure variation at the middle of the pipe calculated by the adjusted five-region turbulence model for the 2-D approach

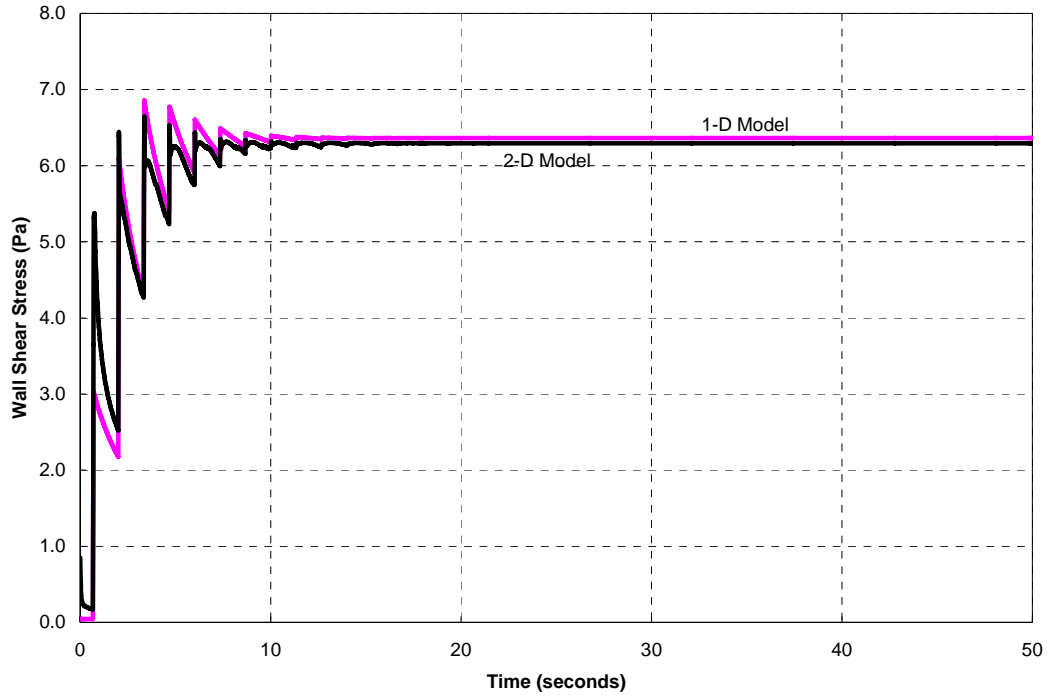


Fig. 5 – Wall shear stress at the middle of the pipe calculated by the adjusted five-region turbulence model for the 2-D approach

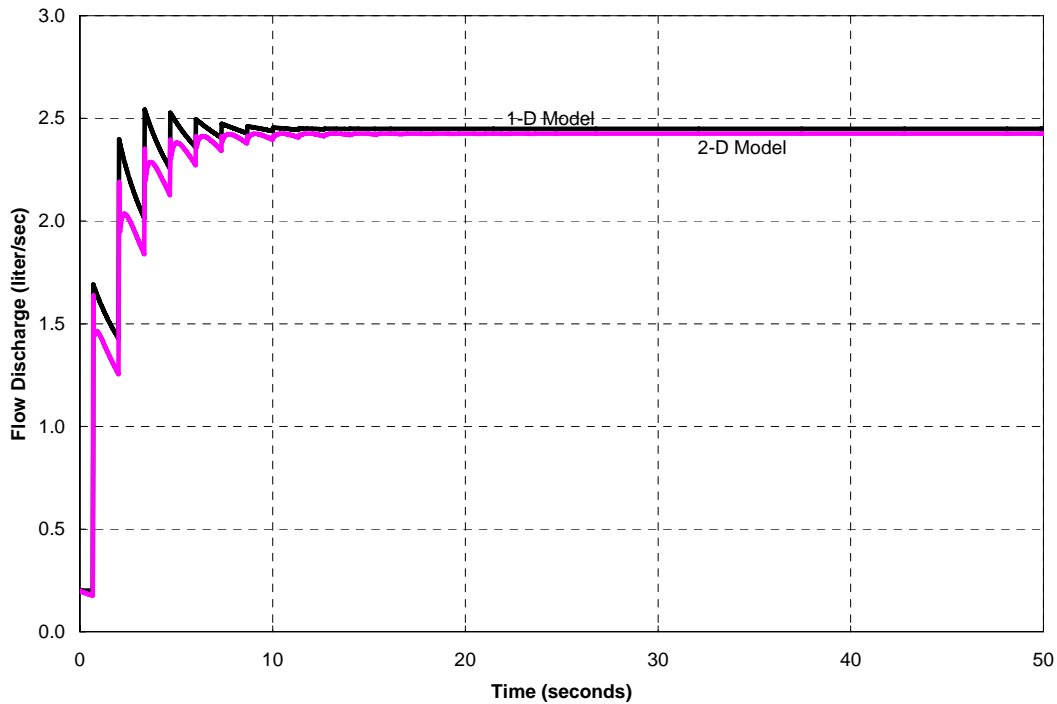


Fig. 6 – Flow discharge variation at the middle of the pipe calculated by the adjusted five-region turbulence model for the 2-D approach

Although the proposed 2-D model with the current five-region turbulence model was not able to accurately predict flow hydraulics, in order to investigate in a crude way the model's capability to simulate the discoloration event, the impacts of the transient event on water turbidity were studied and the results for the 1-D transient model, the proposed 2-D model (with the standard five-region turbulence model), and a 1-D quasi-steady model (using EPANET) are compared with the measured data at the valve position by Boxall et al. (2003) in Fig. 7. Specifically, the Figure represents the time-variations of the numerically calculated cross-sectionally averaged turbidity at the valve position compared with the field data. Overall, the results not only suggest a progressive increase in water turbidity along the pipeline, but also demonstrate an exponential decay in turbidity immediately after an initial sharp increase. Although the comparisons clearly show not only the potential capability of the 2-D approach but also display a fairly good agreement between both 1-D and 2-D predictions and field data, the transient 1-D approach offers a better representation for water turbidity. Moreover, both the quasi-steady and transient 1-D models show a faster rate for water turbidity decay than the 2-D approach. Considering the standard five-region turbulence model for the 2-D approach, this could be partly interpreted as a consequence of the more accurate prediction of wall shear stresses and the velocity effect in the 1-D model relative to that of the proposed 2-D approach. It should be noted that although there are possible uncertainty relating to the measurement of the pipe roughness, it seems the 1-D approach provides more realistic representation of energy dissipation and shear stresses. Therefore, a better representation of wall shear stress and energy dissipation by a more accurate turbulence model for the 2-D approach could prove an enormous help in realistically representing turbidity at the hydrant.

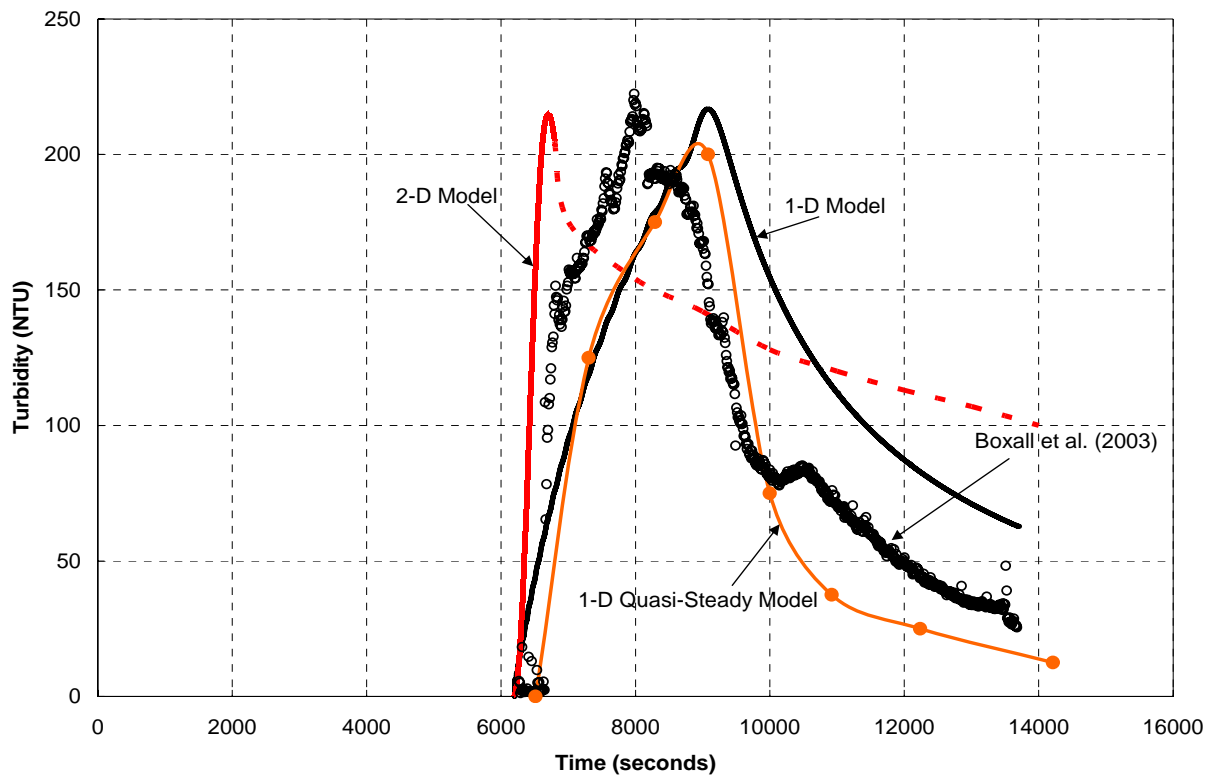


Fig. 7 – 1-D and 2-D models' results for turbidity at the hydrant calculated by the standard five-region turbulence model for the 2-D approach

Calibrating the model prediction with field data, the parameters of the discoloration model in (14) and (15) were estimated for both models. Clearly, all that can be said is that the corresponding parameters in both the 1-D and 2-D models are approximately of the same order of magnitude, except for the two parameters  $C_{max}$  and  $k$ . The differences between the values of these two parameters in those models are almost certainly due to the differences in model predictions for wall shear stress and velocity profile representation. Moreover, considering the fact that the pipeline system in this study is relatively old (Boxall et al., 2003) and extremely rough (with absolute wall roughness of 5.5 mm), the Darcy-Weisbach formula and consequently the 1-D approach, produces higher and probably more accurate predictions of wall shear stresses than the standard five-region turbulence model in the 2-D approach.

It is worthwhile mentioning that the calibration procedure in this study was performed using a trial and error approach. However, due to the strong dependency of the model parameters on system properties, and also on the flow parameters, such a calibration approach is cumbersome and inefficient. A more systematic and automatic calibration approach is recommended for future use of the discoloration model.

It should be mentioned that although the discoloration model was generally successful in explaining the water turbidity at the hydrant, the model's parameters depend not only on system characteristics but also on the flow parameters. This strong dependency renders the calibration of the model's parameters problem-dependent and therefore challenging to determine. The data available to date must be viewed as primarily a calibration set, and more sophisticated and continuing verification must await more comprehensive field measurements.

## 8. CONCLUSIONS

Transient events create sudden changes in flow conditions and consequently produce large aggressive shear forces at the pipe wall. If these forces are exceeded the strength of the accumulated layers, they can cause the particles at the pipe wall to be resuspended and consequently conveyed with the bulk flow.

This paper studied 1-D and 2-D numerical simulations of discoloration events in a WDS. Using a mass transport concept and considering all transport mechanisms (including advection, diffusion, and dispersion), turbidity of water was modeled by a 2<sup>nd</sup>-order PDE, which is then coupled with the continuity and momentum equations for flow. A numerical approach including an implicit/explicit FDM and a fixed grid MOC were used to numerically integrate the governing equations for unknown flow parameters in which the eddy viscosity and diffusion coefficients were determined by the standard five-region turbulence model. Finally, the models' results for a real WDS including a constant head reservoir, a pipeline, and a valve were compared with the corresponding field data reported by other researchers.

Although there were overall agreements among the three sets of results supporting the basic validity of the proposed 2-D model, the results for the hydraulic model exposed a shortcoming of the five-region turbulence model in predicting shear forces at the pipe wall. The case study here includes an old and extremely rough pipeline and the five-region turbulence model was not able to account for the effect of wall roughness on energy dissipation.

Unfortunately, although the modeling approach is consistent with the variable strength concepts for describing the erosion of cohesive estuarine mud and in-sewer deposits with cohesive properties (Boxall et al., 2001), the various parameters ( $C_{max}$ ,  $P$ ,  $n$ ,  $b$ ,  $k$ , and  $\tau_s$ ) are

strongly problem dependent and they must be determined through a careful calibration procedure. In this study, a trial-and-error based calibration procedure was performed to estimate the magnitude of the model parameters. Although the procedure was successful for the current case study, due to a strong dependency of the parameters on flow conditions and system properties, a more sophisticated procedure using an evolutionary algorithm such as GA is recommended for future work.

## 9. REFERENCES

- Abbott, M. B., and Minns, A. W., (1998). *Computational Hydraulics*, Brookfield Vt. Andershot, England, 2<sup>nd</sup> Ed.
- AWWARF, (1996). *Internal Corrosion of Water Distribution Systems*, American Water Works Association Research Foundation, 2<sup>nd</sup> Edition, Denver, USA.
- Baylis, J. R., (1926). "Prevention of Corrosion and 'red water'", *J. of American Water Works Association*, 15:598.
- Boxall, J. B., Skipworth, P. J., and Saul, A. J., (2001). "A Novel Approach to Modeling Sediment Movement in Distribution Mains Based on Particle Characteristics", *Water Software Systems*, Vol. 1, PP. 263-273.
- Boxall, J. B., Skipworth, P. J., and Saul, A. J., (2003). "Aggressive Flushing for Discoloration Event Mitigation in Water Distribution Networks", *Water Science and Technology: Water Supply*, Vol. 3, No. 1-2, PP. 179-186.
- Hoven, V. D. T., and Vreeburg, J. H. G., (1992). "Distribution System Analysis by Continuous Monitoring and Network Calculation", *Water Supply*, Vol. 10, No. 1, PP. 117-124.
- Hoven, V. D. T., Van Der Kooij, D., Vrebutg J., and Brink, H., (1994). "Methods to Analyze and to Cure Water Quality Problems in Distribution Systems", *Water Supply*, Vol. 12, No. 3-4, PP. 151-159.
- Kuch, A., and Sontheimer, H., (1986). "Intationare Korrosion-Ein Ursache der Rostwasserbildung in Wasserverteilungsnetzen", *Gwf-Wasser/Abwasser*, Vol. 127, No. 12, PP. 621. (Cited in Smith et al., 1999).
- Kita, Y., Adachi, Y., and Hirose, K., (1975). "Periodically Oscillating Turbulent Flow in a Pipe", *Bulletin of the JSME*, 23(179), PP. 656-664.
- Kuch, A., (1984). "Investigations of the Reduction and Re-Oxidation Kinetics of Iron (III) Oxide Scales Formed in Waters", *Corrosion Science*, Vol. 28, No. 3, PP. 221-231.
- Rodi, W., (1993). *Turbulence Models and their Application in Hydraulics; A State of the Art Review*, A. A. Balkema, Rotterdam, Netherlands, 3ed Edition.
- Smith, S. E., Colbourne, J. S., Holt, D. M., Lloyd, B., and Bisset, A., (1996). "An Examination of Nature and Occurrence of Deposits in Distribution System and Their Effect on Water Quality", *Proceeding of Water Quality Technology Conference*, AWWA, Denver, 1995.
- Smith, S. E., Bisset, A., Colbourne, J. S., Holt, D. M., and Lloyd, B. J., (1997). "The Occurance and Significance of Particles and Deposits in a Drinking Water Distribution System", *J. of New England Water Works Association*, Vol. 111, No. 2, PP. 135.
- Smith, S. E., Ta, T., Holt, D. M., Delanoue, A., Colbourne, J. S., Chamberlain, A. H. L., and Lloyd, B. J., (1999). "A Pipeline Testing Facility for the Examination of Pipe-Wall Deposits and Red-Water Events in Drinking Water", *Water and Environmental Management, J. of CIWEM*, Vol. 13, No.1, PP. 7-15.

- Vardy, A. E., and Hwang, K. L., (1991). "A Characteristic Model of Transient Friction in Pipes", *J. of Hydraulic Research*, Vol. 29, No. 5, PP. 669-684.
- Wagner, I., and Kuch, A., (1984). "The influence of Water Parameters on Corrosion Rate, Scale Deposition, and Iron (II) Uptake in Unprotected Iron Pipes", *Water Supply*, Vol. 2, No. 3-4, Special Subject 11, 1.
- Woodward, C. A., Ta, C. T., Colbourne, J., and Holt, D., (1995). "Behaviour of Particles in a Large Scale Experimental Pipe System", *Proc. Water Quality Technology Conference*, AWWA, New Orleans, LA, PP. 641-658.
- WRc, (1989). *Removing loose deposits from water mains: Operational Guidelines*, WRc Wiltshire, UK.
- Zhao, M., and Ghidaoui, M. S., (2003). "An Efficient Solution for Quasi Two-Dimensional Water Hammer Problems", *J. of Hydraulic Engng.*, ASCE, Vol. 129, No. 12, PP. 1007-1013.